P. Caron, O. Lavigne
(Onera)

E-mail: pierre.caron@onera.fr

Recent Studies at Onera on Superalloys for Single Crystal Turbine Blades

Recent alloy development works conducted at Onera for single crystal turbine blade applications succeeded in identifying specific nickel-based superalloys suited for very high temperature applications in aircraft engines and for land-based gas turbine applications in a highly corrosive environment. Various studies concerning the mechanical behavior of such single crystal superalloys showed significant effects of the chemical, microstructural and physical characteristics on the deformation mechanisms, as well as on the creep, tensile and fatigue strength of these materials. Finally, the interactions between some SC superalloys and their protective coatings were investigated, in order to evaluate their influence on the mechanical properties and on the microstructural changes in the coated alloy.

Introduction

Single crystal (SC) turbine blade technology is widely used today in modern high performance aero-engines and land-based gas turbines. The use of SC high pressure turbine blades and vanes made of nickel-based superalloys contributes efficiently to the continuous performance increase of these engines in terms of power and thermal efficiency. For thirty years Onera has actively accompanied the French aero-engine manufacturers Snecma and Turbomeca in the introduction of single crystal blade alloys into their new engines, through the development of new superalloy compositions and by performing a number of studies aimed at improving the understanding of the complex relationships between the chemistry, the process, and the properties of these alloys. This paper gives some examples of the recent work performed at Onera in these domains over the last ten years.

Alloy development

MC-NG, a fourth generation superalloy for very high temperatures

Since the introduction in late 1970s of the first SC turbine blades in the high pressure section of aircraft gas turbine engines, the compositions of the nickel-based superalloys suited for these applications have continuously evolved with the aim of increasing their mechanical strength and temperature capability. The chemistries of the first generation alloys were derived from those of existing nickel-based superalloys previously designed for conventional casting or directional solidification processes, leading to equiaxed or columnar grained microstructures respectively. The suppression of the grain boundaries, preferential <001> crystallographic growth orientation and optimized chemical compositions were the main factors for the significant improvement of the creep and fatigue properties, which determine the life of the components. During the 1980s, Onera has participated in, or conducted, several alloy development programs leading to the introduction of first generation SC superalloys in Snecma and Turbomeca gas turbine engines. The AM1 superalloy (table 1) is now used in the M88-2 Snecma engine that powers the Rafale fighter as material for high pressure gas turbine blades and vanes, as well as in the TP400 engine of the Airbus A400M military airplane and in the SaM146 engine that powers the Sukhoi Superjet 100 regional airplane. AM3 and MC2 alloys were successively chosen by Turbomeca for manufacturing the high pressure SC turbine blades of helicopter engines.

Box 1 - Single crystal nickel-based superalloy microstructure

Single crystal blades made of high performance nickel-based superalloys are produced by investment casting in a directional solidification furnace and by using a grain selector or a seed of desired crystallographic orientation placed at the bottom of the mold. After solution and aging heat treatments, the microstructure of a SC nickel-based superalloy is made of an austenitic nickel rich γ matrix strengthened by a high volume fraction (up to 70 vol.%) of γ'-Ni$_3$Al ordered precipitates with a cubic L1$_2$ structure. The γ' precipitates are homogeneously distributed in the γ matrix and have sizes of less than 1 μm (figure B1-01). The γ' phase is highly coherent with the γ matrix, however with a small mismatch between the lattice parameters of the two phases defined as $\delta = 2(a_{\gamma'} - a_{\gamma})/(a_{\gamma'} + a_{\gamma})$, where $a_{\gamma'}$ and a_{γ} are the respective lattice parameters of the γ' and γ phases. The high volume fraction of precipitates associated with the strong solid solution strengthening of both γ and γ' phases, due to multiple alloying, confer to these alloys their outstanding mechanical strength over a wide range of temperatures.

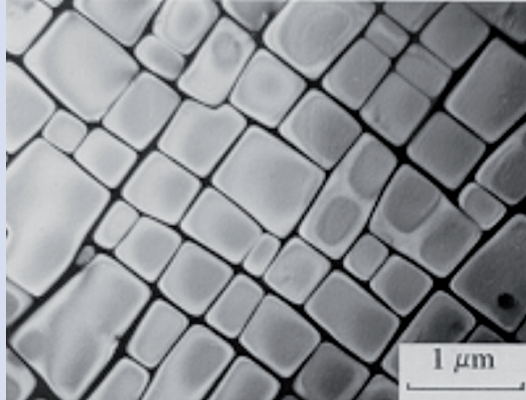Figure B1- 01 - γ-γ' microstructure of a nickel-based SC superalloy.

The first original modification of the SC superalloy chemistry was the introduction of rhenium (Re). This refractory element introduces significant creep advantages over first generation alloys due to solid solution strengthening effects, but above all due to its low diffusion rate, which slows down all the thermally activated mechanisms controlling the high temperature deformation and damage mechanisms. Typical second generation SC superalloys containing about 3 wt.% Re, are René N5, CMSX-4 and PWA1484, which were respectively developed in the USA by General Electric, the Cannon Muskegon Corporation and Pratt & Whitney. These three alloys are widely used today as turbine blade and vane materials in a variety of aircraft engines, as well as in land-based gas turbine engines for power generation. Further increase of the Re concentration, up to values close to 6 wt.%, led to the development of third generation SC superalloys such as René N6 by General Electric and CMSX-10 by the Cannon Muskegon Corp. [1]. However, the addition of Re is not a panacea, since it entails some drawbacks, such as a high cost, limited availability, proneness to casting defects, increase of the density and higher proneness to deleterious topologically close-packed (TCP) phase precipitation.

An alloy development program was thus undertaken in the 1990s at Onera, in order to identify a material with high temperature properties equivalent to those of third generation single crystal superalloys, but with a lower density and no propensity to form TCP phase precipitates. Such an alloy was thought to be particularly well suited for applications in small helicopter engines, where an emergency regime could occur and cause rapid temperature increase for a short time, but at temperatures above 1150°C. Under these conditions, the blade material must have sufficient creep strength to avoid excessive lengthening of the airfoil. In order to attain these objectives, the deci-

sion was made to develop new alloy compositions with rhenium, but also adding ruthenium (Ru), a refractory element with a density of half that of rhenium [2, 3].

Since the strengthening γ' phase dissolves progressively when the temperature increases above 1000°C, a challenge when designing new alloys was to raise the temperature at which the γ' phase completely disappears, i.e. the γ' solvus temperature. More than twenty experimental alloys were thus defined, then melted and cast as SC bars in order to assess their physical, mechanical and environmental properties. Alloy design was performed by taking into account the data bases and the experience previously acquired at Onera. Thus, time-saving formulae deduced from the analyses of these data bases were used to estimate the γ' solvus temperature for the alloy composition, as well as the density and the lattice parameter mismatch between the γ and γ' phases. The New PHACOMP method, devised on the basis of molecular orbital calculations of the electronic structure [4], was used to predict the formation of TCP brittle phases. An additional objective was to achieve an acceptable resistance to the combustion gas environment, which is highly oxidizing and corrosive. Small contents of hafnium (Hf) and silicon (Si) were thus added to the experimental alloys, in order to improve their high temperature oxidation resistance, as previously shown for the AM1, AM3 and MC2 alloys [5]. Moreover, the levels of molybdenum (Mo) and titanium (Ti) were kept low, in order to preserve the environmental resistance. The chemical compositions of three of the most relevant experimental alloys, MC534, MC544 and MC653, are reported in table 1, together with those of the reference first generation MC2 superalloy and the third generation CMSX-10M and René N6 SC alloys.

Alloy	Ni	Co	Cr	Mo	W	Re	Ru	Al	Ti	Ta	Others
MC2	Bal.	5	8	2	8	-	-	5	1.5	6	-
MC653	Bal.	-	4	4	5	3	4	5.8	-	6	0.1 Si; 0.1 Hf
MC544 (MC-NG)	Bal.	-	4	1	5	4	4	6	0.5	5	0.1 Si; 0.1 Hf
MC653	Bal.	-	4	1	6	5	3	5.3	1	6.2	0.1 Si; 0.1 Hf
CMSX-10M	Bal.	1.75	2	0.4	5.4	6.5	-	5.78	0.24	8.2	0.08 Nb
René N6	Bal.	12.5	4.5	1.1	5.7	5.3	-	6	-	7.5	0.15 Hf; 0.05 C; 0.004 B
AM1	Bal.	6.5	7.8	2	5.7	-	-	5.2	1.1	7.9	-
MC-NG-LGP	Bal.	-	4	1	5	4	4	5.52	0.46	4.6	0.1 Si; 0.1 Hf
MC-NG-Mod	Bal.	-	4	1	4	4	5	4.8	1.2	7.7	0.1 Si; 0.1 Hf
MC-NG-Co	Bal.	10	4	1	5	4	4	6	0.5	5	0.1 Si; 0.1 Hf

Table 1 – Compositions of SC superalloys (wt. %)

Figure 1 - Changes with temperature of the γ' volume fraction in three SC superalloys.

Figure 2 - Typical creep curves of <001> single crystal superalloys at 1150°C and 100 MPa.

The objective of increasing the γ' solvus temperature compared to MC2 was successfully attained, as illustrated in figure 1 for the MC544 and MC653 alloys. At 1150°C, the residual amount of the γ' phase is still more than 55% in the new alloys, whereas it decreased below 45% in MC2. This increase in the residual fraction of the γ' phase is thought to be the main reason for the corresponding dramatic improvement in creep strength at 1150°C, illustrated by the creep curves of single crystal specimens oriented within 5° of a <001> crystallographic direction (figure 2), even if this does not exclude other beneficial effects resulting from high concentrations in refractory elements. For rotating components, such as turbine blades, the alloy density is a crucial parameter and the creep strength must be considered on a specific strength basis, to evaluate properly the potential of the new alloy. An effort was therefore made, when developing the new alloys, to limit their density. A good balance of the Re and Ru content was shown to be an efficient way to attain this objective, while maintaining a specific creep strength comparable to that of third generation alloys, but with a lower density. The MC544 was further selected for a more complete evaluation on an industrial scale at Snecma and Turbomeca, under the name of MC-NG (MonoCristal-Nouvelle Génération) [6]. This alloy shows a unique combination of properties, with a reasonable density of 8.75g.cm^{-3}, a satisfying environmental resistance and no propensity to form brittle TCP phase precipitates after exposure to high temperatures. This work shows that there is a promising alternative to the third generation superalloys for increasing the temperature capability of the SC turbine blade without being penalized by an excessive density or by microstructural instabilities.

Mechanical behavior and deformation mechanisms

In order to satisfy the increasing mechanical strength requirements for advanced SC blades, the nickel-based superalloys tailored for these applications must have adequate tensile, creep and fatigue behaviors. It is therefore of the utmost importance to carefully analyze the influence of various chemical and microstructural parameters on these properties, to efficiently develop new alloy compositions, to optimize their microstructures and to have a good description of the mechanical behavior of these materials under various stress and temperature conditions. A number of studies have thus been conducted at Onera in this field of research, addressing various aspects of the relationships between the chemistry, microstructure, physical properties and mechanical behavior of different SC superalloys.

Creep behavior at an intermediate temperature

Even though knowledge of the high temperature (T > 900°C) creep behavior of such materials is essential, since it concerns blade airfoils subjected to the highest thermal solicitations, the intermediate temperature creep behavior (T ≈ 750°C) was also investigated, since it concerns parts of the blade such as the platform and the bottom of the airfoil, where localized stress concentration due to geometrical effects (cooling channel system, sharp section changes) may induce local creep damage. Figure 3 compares the tensile creep curves obtained at 760°C and 840 MPa for SC specimens of the AM1, MC534, MC-NG, CMSX-10M and René N6 superalloys [13]. All the SC specimens have orientations within 5° of a <001> direction. The differences in creep behavior between the various alloys cannot therefore be attributed to an anisotropy effect. MC534 is an experimental new

generation alloy containing Re and Ru additions and a relatively high level of Mo, in order to obtain a large lattice parameter mismatch (table 1) [2]. MC-NG, CMSX-10M and René N6 creep curves are characterized by high amplitude of the primary creep deformation, which varies from about 3 to 10%. The secondary creep rate increases with the primary creep strain and the creep curves end with a short tertiary stage. The primary creep amplitude is dramatically smaller for AM1 and MC534, less than 0.25%. The secondary creep stage is quite short and the main part of the creep life corresponds to a long tertiary creep stage. However, the creep rupture life of AM1 is about ten-time longer than that of MC534. All of these alloys have similar γ/γ' microstructures, but with various chemistries, γ' precipitate sizes and lattice mismatches. The effects of these parameters have therefore been analyzed, in order to explain the differences in creep behavior.
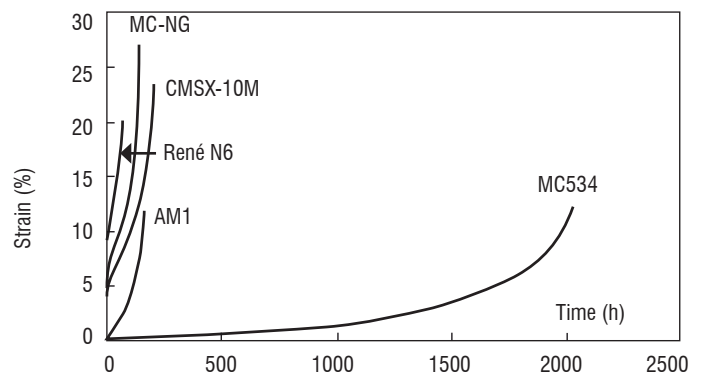

Figure 3 - Creep curves at 760°C and 840 MPa of various nickel-based <001> SC superalloys.

J O U R N A L AerospaceLab   Issue 3 - November 2011 - Recent Studies at Onera on Superalloys for Single Crystal Turbine Blades

AL03-02   4

At 760°C and 840 MPa, AM1 exhibits optimal creep strength with a γ' precipitate size of 480 nm (figure 5a). Decreasing the γ' precipitate size induces an increase in the primary creep extent and a reduction in stress-rupture life. Such a phenomenon, previously observed for the CMSX-2 SC alloy [14], is associated with a change in the deformation mechanism. For a given γ' phase volume fraction, the mean distance between the precipitates, i.e. the γ matrix channel width, decreases with the γ' precipitate size. By-passing of γ' particles by the Orowan mechanism, which controls bowing of perfect a/2<110> matrix dislocations between the precipitates, becomes more difficult when the γ channel width decreases and the γ' cutting mechanism by a/3<112> superpartial dislocations is therefore promoted. The cutting mechanism, which operates in a heterogeneous manner, leads to a faster creep rate and a higher primary creep amplitude than the more homogeneous mechanism involving multiple a/2<110>{111} slip within the γ matrix. However, increasing the γ' size, and then the γ channel width too much, facilitates the bowing of matrix dislocations between the precipitates and therefore decreases the creep strength. The effect of γ' size variation is somewhat different in the case of MC-NG, where <112>{111} slip operates during primary creep for γ' sizes within the range 220-480 nm, but with different levels of heterogeneity. The larger the γ' size is, the wider the γ channel, the more homogeneous the deformation and the smaller the primary creep amplitude.
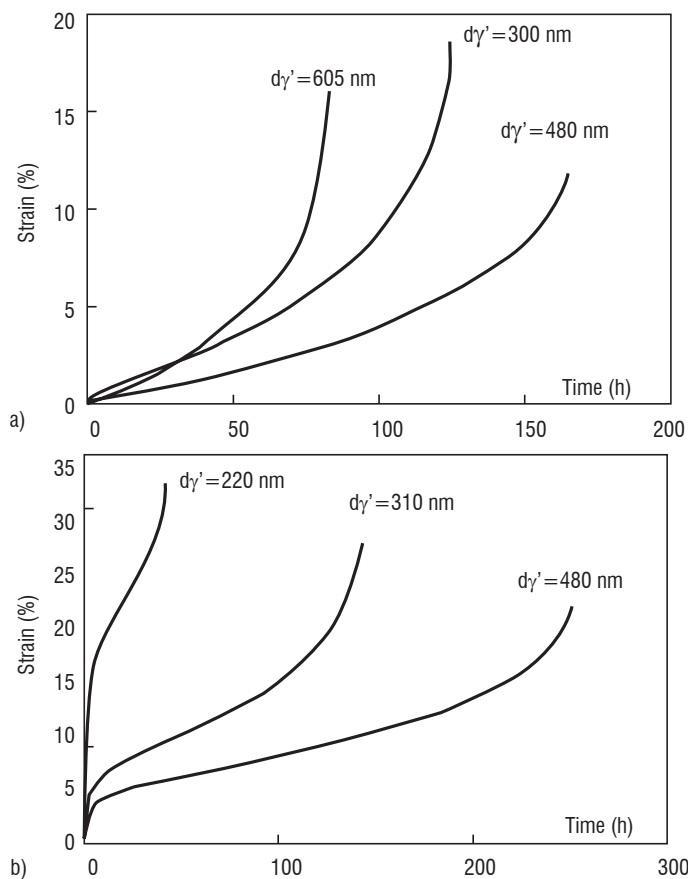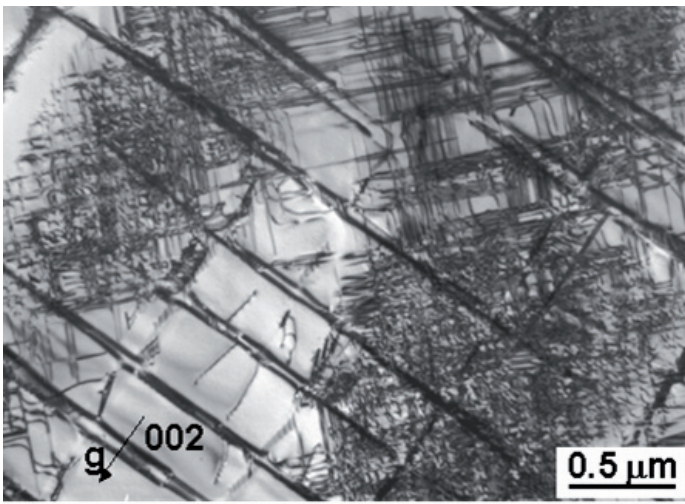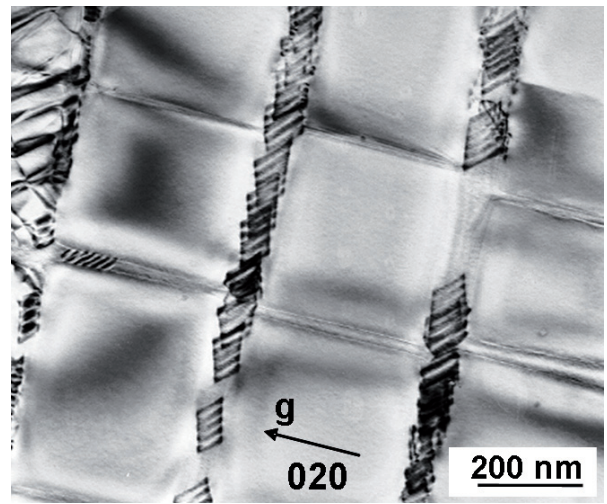
However, the effect of the γ' size cannot explain the differences in creep behavior at 760°C observed between AM1 and MC-NG alloys with the same size of γ' precipitates, i.e. 480 nm or 300 nm (figure 4). Analysis of the solid solution strengthening effect in both phases of the two alloys shows that the γ phase is stronger in MC-NG than in AM1 and inversely that the γ' phase is stronger in AM1 than in MC-NG [13]. Moreover, the γ' phase of AM1 is characterized by a higher value of the antiphase boundary (APB) energy than that in MC-NG, due to its higher level of Ti and Ta. This makes the shearing of the γ' precipitates by matrix dislocations more difficult. All these differences combine to promote an easier a/2<110> dislocation glide in the γ channels of AM1 and to facilitate the shearing of γ' precipitates in MC-NG instead of matrix deformation, as observed experimentally [13].

The difference in creep behavior at 760°C between MC-NG and MC534 alloys was inferred to be due to the high amplitude of the lattice mismatch, measured at - 14.2 x 10^{-3} for MC534 at 760°C, in comparison to the value of - 0.5 x 10^{-3} measured for MC-NG [13]. The γ-γ' mismatch measurements were performed by means of high-energy X-ray diffraction at the beam line ID 15A of the ESRF (European Synchrotron Radiation Facility, Grenoble, France). This high value of δ in MC534 results mainly from the much higher level of Mo, which partitions preferentially to the matrix and significantly increases its lattice parameter. Calculations showed that the coherency stresses generated by this misfit add to the applied stress in the channels normal to this external stress [15]. In MC534, transmission electron microscopy (TEM) observations show that the spreading of the matrix dislocations is strongly promoted in the horizontal channels as soon as the external stress is applied, leading to a high density of dislocations at the γ-γ' interfaces normal to the stress axis (figure 5a). At the same time, the mobility of the matrix dislocations is much lower in the vertical channels, where the applied stress is not assisted by the coherency stresses, as is evidenced by the decorrelated movement of Shockley partial dislocations, with the creation of numerous stacking faults (figure 5b) [16]. Stacking faults in the γ phase were also observed in other Ru-bearing alloys [17-19]. These observations suggest that Ru addition decreases the stacking fault energy (SFE) of the γ matrix. However, no stacking faults were observed within the γ channel of MC-NG, which shows that an analysis based only on SFE considerations cannot explain the difference in creep behavior between the MC534 and MC-NG alloys. In any case, the dense dislocation networks rapidly formed at the γ-γ' interfaces act as obstacles to the motion of dislocations in the matrix and also against the shearing of the precipitates, which explains the very limited extent of primary creep for this alloy in comparison to MC-NG. High amplitude of deformation during the primary creep stage, as observed for MC-NG, René N6 or CMSX-10M, penalizes their stress-rupture life in comparison to that of MC534, since the level of stress at the beginning of the secondary creep stage increases proportionately to the primary creep strain.

Figure 4 - Creep curves at 760°C and 840 MPa for a) AM1 and b) MC-NG <001> single crystals with various γ' precipitate sizes.

AerospaceLab JOURNAL Issue 3 - November 2011 - Recent Studies at Onera on Superalloys for Single Crystal Turbine Blades

AL03-02   5

a) Dislocation networks at the γ-γ' interfaces normal to the stress axis

b) Stacking faults within the vertical γ phase channels

Figure 5 - Dislocation structures in MC534 after creep at 760°C and 840 MPa (foil normal to the [001] stress axis, t = 4.6 h, ε = 0.08%).

Creep behavior at high temperatures

A strong microstructural change in the SC superalloys during tensile creep at high temperatures (T > 900°C) is the directional coalescence of the γ' precipitates, leading to a rafted γ-γ' microstructure normal to the <001> tensile axis when the γ-γ' is negative, as is the case for all industrial alloys. This phenomenon results from the combined effects of centrifugal tensile stress, diffusion, γ-γ' coherency stress and γ-γ' elastic modulus misfit. The rate of transition between the cuboidal and the rafted morphology of the γ' particles, as well as the stability of the γ-γ' rafted microstructure, therefore depend on the alloy chemistry and influence the creep behavior. Typical tensile creep curves obtained at 1050°C and 150 MPa for <001> oriented SC specimens of MC2 and MC-NG alloys are compared in figure 6 [20]. The stress-rupture times are almost comparable but the shapes of the curves differ in several points. Primary creep occurs for MC2 as soon as the load is applied while the creep for MC-NG starts with a low creep rate incubation period before primary creep happens. The secondary creep stage is dramatically shorter for MC-NG than for MC2 and the tertiary creep stage therefore begins much earlier. Tertiary creep is however longer in the case of MC-NG, which makes the stress-rupture lives comparable for both alloys.
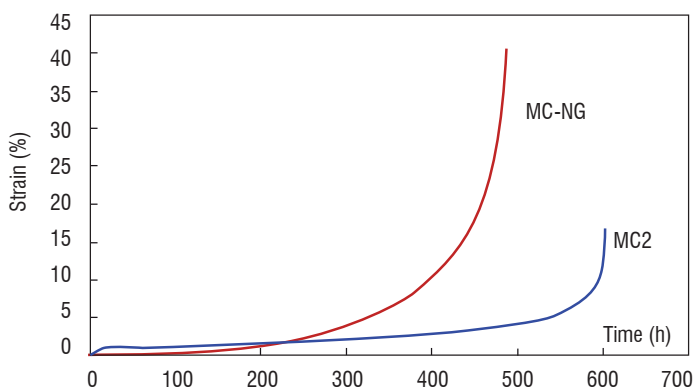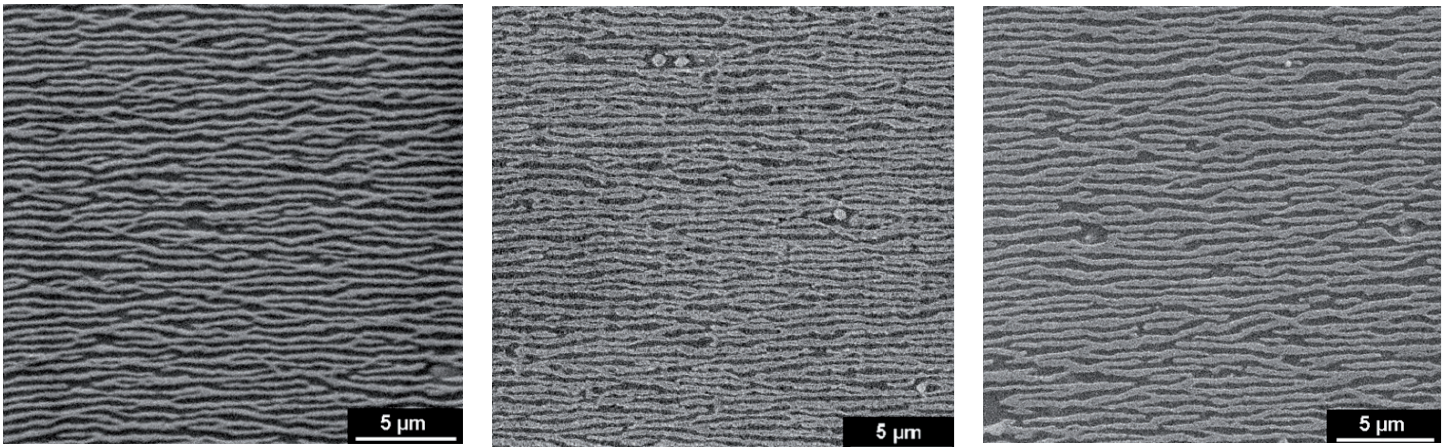

Figure 6 - Creep curves of <001> MC2 and MC-NG SC alloys at 1050°C and 150 MPa.

After 20 hours of creep, scanning electron microscopy (SEM) observations of longitudinal sections of SC specimens show that the γ-γ' rafted microstructure is well established in MC2 (figure 7a), whereas there is no significant change in the initial structure for MC-NG (figure 8a). The primary creep is associated with the cube-raft morphology transition, which is inhibited, or at least delayed, in MC-NG. Correlatively, TEM observations of the dislocation structures show an intense deformation activity in the matrix of MC2 leading to the formation of dense dislocation networks at the γ-γ' interfaces, while very few dislocations are observed in the γ matrix channels of MC-NG. These observations confirm that the oriented coalescence of γ' precipitates is promoted by plastic deformation. After about 120 hours, the secondary creep stage is attained for both alloys, where regular γ-γ' rafted microstructures are stabilized (figure 7b and 8b). After 310 hours, the creep curve of MC-NG has largely entered into its tertiary stage, while the secondary creep stage is still running for MC2. Whereas the γ-γ' rafted microstructure is still regular in MC2 (figure 7c), it is totally destabilized in MC-NG (figure 8c) where a complete γ-γ' topological inversion has occurred. The γ phase, which surrounded the γ' precipitates before the creep test was started, becomes progressively surrounded by the γ' phase as soon as the tertiary creep stage occurs. At the same time, TEM observations show an increased dislocation activity within the γ' phase, parallel to the γ phase deformation. The continuous increase of the creep rate during tertiary creep of MC-NG is associated with the growing activity of the deformation mechanisms in both the γ and γ' phases, resulting from the γ-γ' topological inversion. On the other hand, the long secondary creep stage in MC2 is related to the stability of the γ-γ' rafted microstructure, where the dislocation activity is mainly confined in the γ matrix. Some authors have concluded that the stability of the rafted structure of SC nickel-based superalloys, during creep at high temperatures, increases with the amplitude of the negative γ-γ' mismatch [21, 22]. This argument cannot however be retained to explain the better stability of the γ-γ' microstructure during creep of MC2, compared to that of MC-NG, since the amplitude of the γ-γ' mismatch at 1050°C is slightly higher for MC-NG than for MC2 [20].
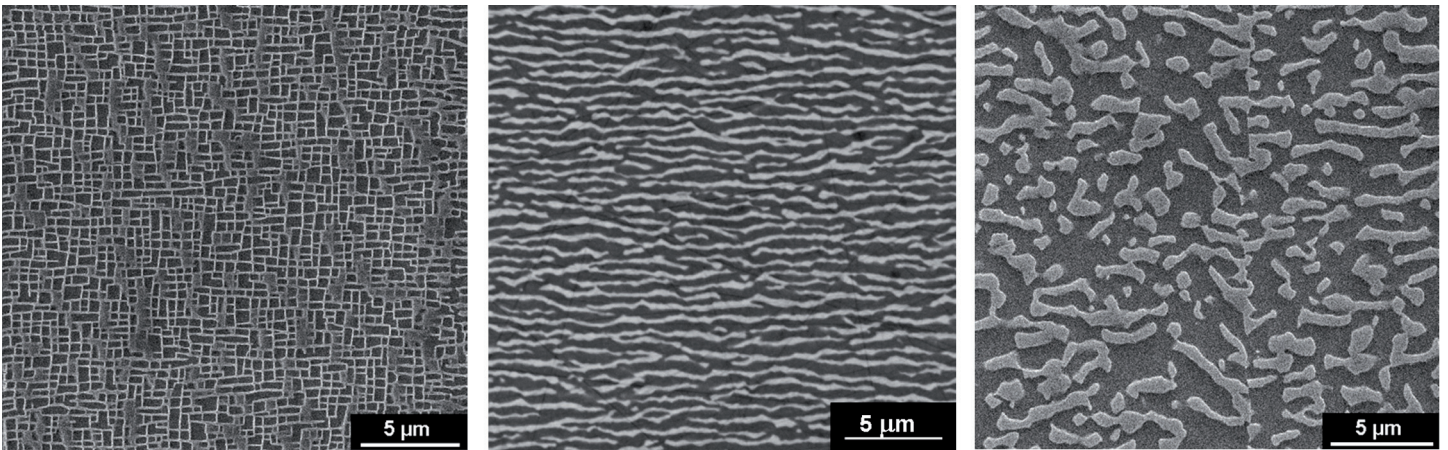
a) t = 20 h, ε = 0.51%   b) t = 123 h, ε = 0.8%   c) t = 314 h, ε = 0.89%

Figure 7 - Changes in the γ-γ' microstructure during creep at 1050°C and 150 MPa of <001> MC2 SC specimens (sections cut parallel to the tensile axis; the darkest phase is the γ' phase).

a) t = 21 h, e = 0.06%   b) t = 120 h, ε = 0.65%   c) t = 310 h, ε = 4.45%

Figure 8 - Evolution of the γ-γ' microstructure during creep at 1050°C and 150 MPa of <001> MC-NG SC specimens (sections cut parallel to the tensile axis; the darkest phase is the γ' phase).

Figure 9 - Evolution of $N_A(γ')$ and strain rate during creep at 1050°C and 150 MPa.

An analysis of the topological inversion phenomenon was performed by measuring the changes over time of the specific connectivity number of the γ' phase $N_A(γ')$, during creep tests at 1050°C and 150 MPa, of AM1, MC2 and MC-NG <001> SC specimens [23]. In the initial state, where the γ phase is fully connected, $N_A(γ')$ is positive and becomes negative when the topological inversion occurs. These measurements were performed on SEM micrographs of interrupted creep specimen longitudinal sections. Area fractions of γ' phase were also measured on samples quenched after heat treatments at 1050°C, 1100°C and 1150°C, to follow the variation with temperature of the γ' volume fraction. Variations of $N_A(γ')$ with creep time are plotted in figure 9, together with the respective creep strain rates.

Alloy	T=1050°C		T=1150°C	
	$F_A(\gamma')$(%)	$N_A (\gamma')(\mu m^{-2})$	$F_A(\gamma')$(%)	$N_A (\gamma')(\mu m^{-2})$
AM1	52.0	-0.081	42.5	+0.105
MC2	44.5	-0.015	39.9	+0.265
MC-NG	62.4	-0.221	48.6	+0.127
MC-NG-LGP	40.4	+0.080	nd	nd
René N6	61.1	-0.093	46.4	+0.133
CMSX-10M	67.3	-0.115	55.2	+0.094

Table 2 - Area fraction and specific connectivity number of the γ' phase after rupture, during creep at 1050°C and 150 MPa and at 1150°C and 100 MPa (nd : not determined).
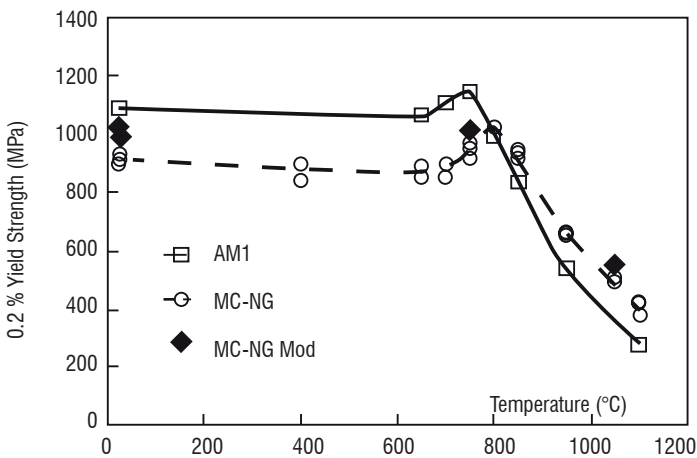

Figure 10 - Variation with temperature of the YS of AM1, MC-NG and MC-NG Mod SC alloys.

In AM1 and MC-NG, the onset of the strain rate increase corresponds to the topological inversion, i.e. to the moment at which $N_A(\gamma')$ becomes negative. In MC2, topological inversion is observed only in the ruptured specimen and is not very pronounced, both γ and γ' phases remaining strongly interconnected. Creep tests have been performed at 1150°C and 100 MPa to check whether γ-γ' topological inversion still occurs under these conditions. The stress rupture life of MC-NG is dramatically longer than that of AM1 and MC2 (about 150 hours instead of less than 20 hours) but, above all, the creep curve of MC-NG at 1150°C has the same shape as those of AM1 and MC2 at 1050°C [23]. Microstructural analyses of stress-ruptured specimens show that $N_A(\gamma')$ remains positive up until rupture in these three alloys, which means that the γ' phase particles are still completely surrounded by the γ phase (table 2). Additional creep tests were performed at 1050°C and 150 MPa on SC of the experimental MC-NG-LGP (low Gamma Prime) alloy, with reduced contents in γ'-former elements compared to MC-NG. This alloy, with a γ' phase fraction close to 40% at 1050°C, did not experience γ-γ' topological inversion at this temperature. Moreover, the comparison of $N_A(\gamma')$ values and the fraction of γ' phase for different alloys shows a strong relationship between the increase in the γ' phase and the growing tendency for topological inversion of the γ-γ' microstructure (table 2).

These experimental results, associated with an analysis of results published in the literature, therefore demonstrate unambiguously that topological inversion of the γ-γ' microstructure of SC nickel-based superalloys during creep at high temperature is inhibited under conditions where the fraction of the γ' phase is lower than about 50%. In alloys where topological inversion occurs, the higher the fraction of the γ' phase is, the earlier this phenomenon occurs during the creep life. This analysis can yield some precious indications for alloy design for a given application, depending on the temperature regime that must be favored, at least as far as creep strength is concerned. Increasing the γ' phase fraction to promote a high creep strength at very high temperatures (T > 1100°C) is not necessarily the most efficient solution to obtain a low creep rate in the high temperature regime (1000°C <T< 1100°C), where the stability of the rafted structure plays an important role. On the other hand, a high volume fraction of the γ' phase may be preferred in the intermediate temperature range (850-950°C), where the γ-γ' microstructure changes slowly and the Orowan resistance governs the creep rate. In any case, it is a huge challenge to optimize the chemistry and the microstructure of such SC superalloys, which must satisfy creep strength requirements over a very large temperature range, typically 700-1150°C, covering the different parts of a turbine blade.

Tensile behavior

The tensile properties of the SC superalloys are not only dependent on their microstructure, but also on their chemistry. Indeed, a survey of the literature reveals that significant tensile strength differences may exist between one alloy and another, especially within the low temperature regime (T < 800°C). An analysis of the influence of the chemistry on the tensile yield strength (YS) of various alloys has therefore been performed, to identify the role of pertinent alloying elements [24]. The tensile yield strengths of <001> AM1, MC-NG and MC-NG Mod SC alloys have been compared within the temperature range 20-1150°C (figure 10). The MC-NG Mod alloy was derived from MC-NG by increasing the Ti and Ta contents at the expense of Al, in order to reinforce the γ'-Ni_3(Al, Ti, Ta) phase, where these alloying elements partition preferentially (table 1). All alloys were aged to produce similar γ' precipitate sizes close to 300 nm, in order to discriminate between possible effects of chemistry and microstructure. The YS of AM1 is significantly higher than that of MC-NG from room temperature up to 750°C and the opposite is observed at temperatures above 800°C. At room temperature and 750°C, the YS of MC-NG Mod is intermediate between those of MC-NG and AM1, which shows the efficiency of increasing the Ti and Ta levels. At 1050°C, the MC-NG Mod YS is slightly higher than that of MC-NG. In the low temperature regime, the matrix dislocations first move through the γ channel by a/2<110>{111} slip, but then the high Orowan strength forces these dislocations to cut the γ' precipitates as pairs bounded by an APB. TEM analyses have shown numerous γ' precipitate shearing events in MC-NG and AM1 tensile specimens after 2% plastic deformation at room temperature, together with a high density of matrix dislocations in the γ channels [25]. In the high temperature regime (T > 800°C), the matrix dislocations propagate between the γ' precipitates by thermally activated glide/climb processes and only few γ' shearing events are observed, which promotes a homogeneous deformation. Under these conditions, the tensile strength is therefore essentially linked to the mobility of the matrix dislocations between the precipitates. Variations in the Orowan stress and in the γ-γ' mismatch were excluded to explain the difference in YS between AM1 and MC-NG in the low temperature regime, since the γ channel width

and the lattice mismatch are comparable in both alloys. The higher YS of AM1 in comparison to that of MC-NG was attributed to the better resistance of the γ' precipitates against shearing. The higher strength of the γ' phase in AM1 compared to MC-NG results from the increased levels of Ti and Ta, which substitute for Al in the γ' phase and which are known to increase its APB energy [26], thus rendering more difficult the shearing of γ' precipitates by pairs of matrix dislocations. The higher YS of MC-NG Mod alloy, which shows Ti, Ta and Al contents close to that of AM1, is in agreement with this conclusion. In the high temperature regime, the better tensile strength of MC-NG compared to that of AM1 was attributed partly to a higher Orowan stress, since γ' solutioning is postponed when the temperature increases, which determines a narrower γ channel in the fourth generation alloy. At 1050°C, typically, the Orowan stress was estimated to be 26% higher for MC-NG than for AM1, taking into account the respective residual amounts of the γ' phase at this temperature. The presence of Re in the MC-NG matrix is also advantageous, since this alloying element has been shown to be the one characterized by the lowest diffusion rate among nickel-based superalloys [27]. This is beneficial for slowing down the climb rate of matrix dislocations, compared to AM1. Finally, the higher solid solution strengthening effect estimated for the MC-NG matrix compared to that of AM1 is an additional argument to explain its greater YS in the high temperature range. Comparison of the data obtained for AM1 and MC-NG with that available for other third and fourth generation SC superalloys confirms our hypotheses.

Box 3 - Impact of γ-γ' rafting on the mechanical properties of SC nickel-based superalloys

Since the γ-γ' microstructure of the SC superalloys changes significantly during creep at high temperatures, it is of the utmost importance to evaluate the impact of such a phenomenon on the other mechanical properties. As an example, MC2 <001> SC specimens were crept during 200 hours at 1050°C and 80 MPa to develop a regular γ-γ' rafted structure before carrying out tensile and low cycle fatigue tests. An effect of the rafting process is to decrease the tensile yield strength (YS) at room temperature (figure B3-01) [28, 29]. TEM observations of unaged and aged tensile specimens tested at room temperature show planar deformation bands with numerous stacking faults within the γ' precipitates (figure B3-02). Outside these bands, deformation operates by a/2<110> dislocation bypass of the γ' particles by the Orowan process. The critical Orowan stress that must be attained to move the matrix dislocations between the precipitates before cutting them is obviously lower in the aged material where the mean spacing between γ' rafts was found to be close to 270 nm, than in the unaged alloy where the γ channel width is about 30 nm. This explains the YS decrease observed at room temperature after aging at 1050°C. A preliminary stress-aging treatment was also shown to decrease the number of cycles to rupture during low cycle fatigue (LCF) tests of MC2 SC specimens at 650 and 950°C [30]. The reduction in YS and easier crack propagation within the γ-γ' rafted microstructure were suggested to be the causes for reduction of the fatigue life of pre-rafted MC2 alloys, compared to the same material containing cuboidal γ' particles.
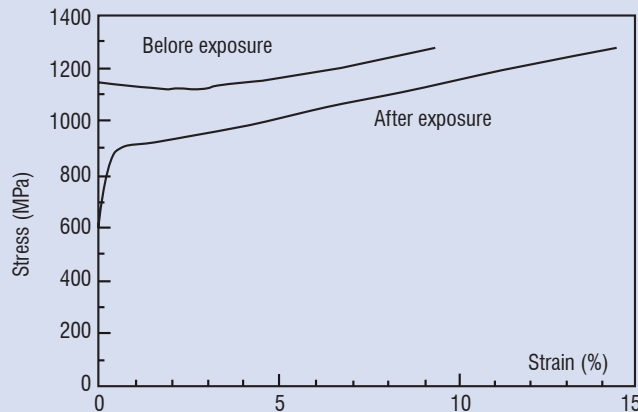

Figure B3-01 – Effect of a 200-hour exposure at 1050°C and 80 MPa on the tensile behavior of the MC2 SC alloy at room temperature.
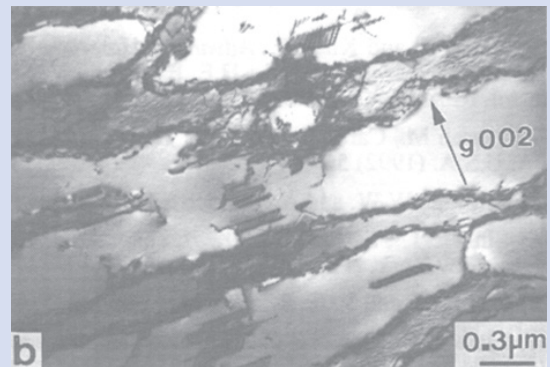

Figure B3-02 – Dislocation structures in tensile MC2 <001> SC specimens strained to 2% at room temperature: a) unaged material, b) aged material.

AerospaceLab JOURNAL — Issue 3 - November 2011 - Recent Studies at Onera on Superalloys for Single Crystal Turbine Blades

AL03-02   9

Interactions between single crystal superalloys and protective coatings

The most advanced high pressure SC turbine blades are protected by a thermal barrier coating (TBC) based on porous ceramic that reduces the temperature of the superalloy substrate and are protected in between by an intermetallic bond coat that ensures a good oxidation resistance and the ceramic coating spallation resistance.

In coated first and second generation SC nickel-based superalloys (Re content between 0 and 3wt. %), interdiffusion phenomena between the substrate and Pt-modified nickel aluminide bond coat create an intermediate zone with a β-NiAl(Pt) matrix, containing precipitates rich in refractory elements (figure 11). In third and fourth generation alloys containing high levels of elements such as Mo, W, Ta, Re and possibly Ru, a deeper secondary reaction zone (SRZ) may develop in the alloy under the primary diffusion zone [31]. Such a SRZ was observed to form in the MC-NG alloy protected by a NiAlPt bondcoat (figure 12) [32]. The SRZ microstructure is cellular with a γ' phase matrix containing elongated γ particles and intermetallic TCP phase precipitates. The driving forces for SRZ formation were suggested to be:

• local changes of composition due to aluminum diffusion towards the superalloy and of nickel and refractory alloying elements in the opposite direction;

• residual stress resulting from the alloy surface preparation prior to coating. Electron backscattered diffraction (EBSD) analysis shows that the cellular transformation leading to the characteristic γ'/γ/TCP phase SRZ microstructure occurs together with the recrystallization of the superalloy affected zone.

Elongated recrystallized grains grow normally to the surface with misorientation relative to the original SC substrate within the [20°, 60°] range (figure 13) [32]. Such high angle misorientations also occur between the grains themselves. The formation of high angle boundaries, on the one hand between the unaffected superalloy and the SRZ and on the other hand between adjacent SRZ grains, is likely to be a weak point in the system with respect to mechanical properties. Moreover, SRZ can extend up to 160 μm into the superalloy (MC-NG aged at 1100°C for 300 hours), thus significantly reducing the alloy load bearing section. Due to its specific microstructure, the SRZ strength is indeed inferred to be much lower than that of the substrate γ-γ' microstructure.
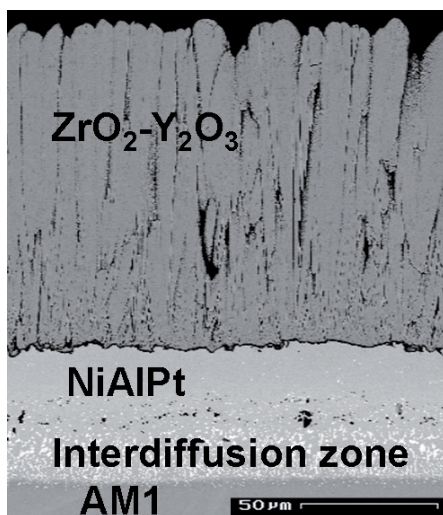

Figure 11 - TBC system on the AM1 SC superalloy: NiAlPt bond coat and ZrO$_2$-Y$_2$O$_3$ EB-PVD (Electron Beam-Physical Vapor Deposition) topcoat.
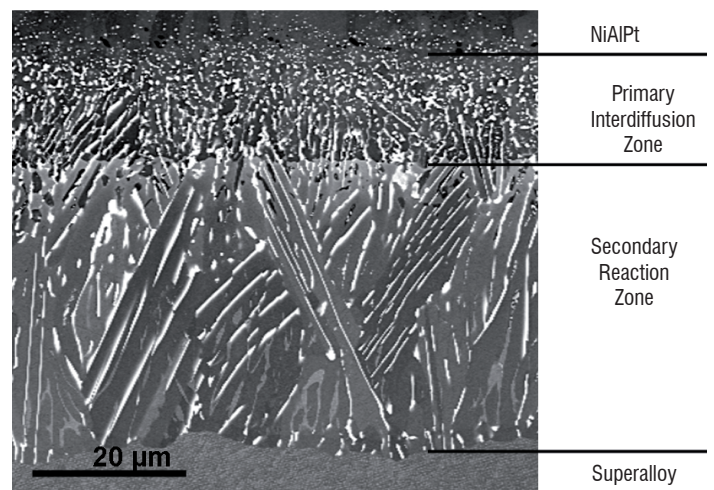

Figure 12 - Microstructure of the diffusion zone in as-coated MC-NG.
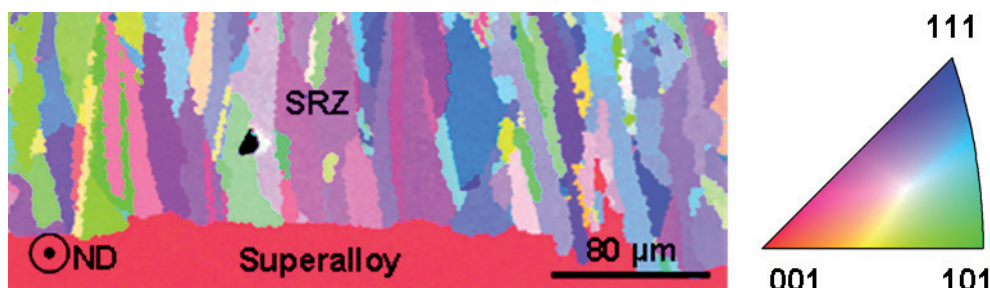

Figure 13 - EBSD inverse pole figure of the SRZ in NiAlPt-coated MC-NG after exposure for 300 hours at 1100°C (ND: sample normal direction) (from [32]).

To estimate the effect of SRZ formation on the creep strength, comparative tests have been performed at 950°C and 300 MPa, at 1050°C and 150 MPa and at 1150°C and 100 MPa, on bare and NiAlPt-coated <001> MC-NG SC specimens. The applied load was determined by taking into account the section of the specimen gauge before coating. The thickness of the SRZ was about 40 μm in the as-coated material and increased to about 75 μm after 204 hours at 950°C. After creep at higher temperatures, it becomes difficult to discriminate between the primary diffusion zone and the SRZ. The total depth of the diffusion zone has increased from 50 μm to 140 μm after 199 hours at 1050°C, and to 110 μm after 62 hours at 1150°C. Considering that the creep resistances of both primary and secondary diffusion zones are significantly lower than that of the γ-γ' microstructure, the true stress acting on the load bearing unaffected alloy was determined at the beginning and at the end of the creep tests, by taking into account the total thickness of the interdiffusion zone. The stress-rupture lives of coated MC-NG are reported in the Larson-Miller diagram presented in figure 14, as a function of the nominal stress (without any section correction) and also as a function of the stress acting on the unaffected alloy section at the beginning and at the end of the corresponding tests. For the sake of comparison, a Larson-Miller curve for the bare MC-NG alloy is reported in this diagram. Without any stress correction, it appears clearly that the presence of the coating significantly reduces the stress-rupture life of MC-NG. With the corrected values of the stress, the stress-rupture life of the coated material is comparable to that of the bare alloy.
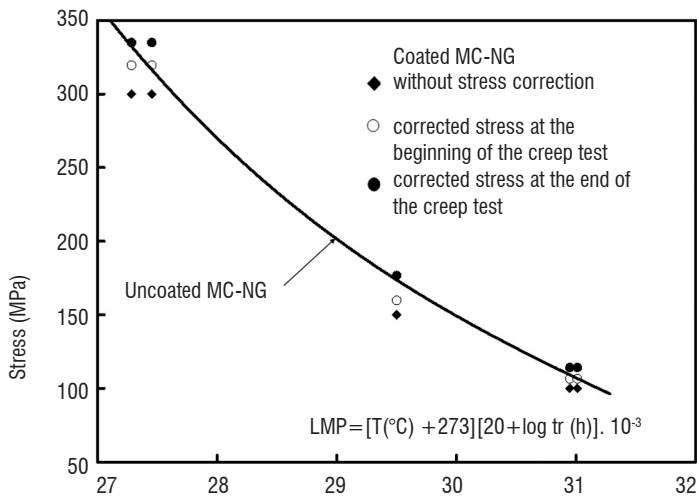

Figure 14 - Larson-Miller diagram for stress-rupture life of MC-NG.

The SEM micrograph in figure 15 illustrates the damage experienced in the SRZ after 199 hours of creep at 1050°C and 150 MPa. Microcracks initiate and propagate within the SRZ, along the grain boundaries. Except for the region very close to the fracture surface, i.e. in the necked portion of the specimen, these cracks never propagate into the unaffected superalloy. The SRZ is therefore a poor strength zone, which is penalized by its recrystallised structure rather than by its celular microstructure or by the presence of TCP phase particles. The SRZ depth is the pertinent parameter required to estimate the deleterious effect of this microstructural instability. Depending on the local section of the single crystal blade, this phenomenon can have a more or less significant effect on the creep behavior of the component.

The strain-controlled LCF behavior of NiAlPt-coated MC-NG <001> SC specimens was investigated at 650 and 950°C, to check whether SRZ can initiate cracks causing premature failure of the material,

compared to the bare case [32]. At 650°C, the number of cycles to failure is adversely affected by the presence of the aluminide coating, especially at the lowest applied stress level (figure 16). The reduction of the load bearing cross section due to SRZ formation is not sufficient to explain this LCF strength decrease. Actually, cracks start in the brittle NiAlPt layer and not in the SRZ, then follow the grain boundaries within the SRZ and continue within the superalloy (figure 17). This explains the resulting loss of LCF strength. At 950°C, i.e., above its ductile-to-brittle transition temperature, the aluminide coating is no longer brittle and is able to accommodate the strain by creep deformation. The cracks leading to the rupture start at casting porosity, as typically observed in uncoated specimens. In this case, the slight decrease in the LCF strength was shown to be mainly due to the reduction in the load bearing cross section. Under severe laboratory test conditions, the NiAlPt layer was strongly deformed and therefore contained numerous cracks propagating within the SRZ. Contrary to what was observed at 650°C, the cracks did not cross the boundary separating the SRZ and the γ-γ' superalloy, but rather split along this interface (figure 18). This explains the limited deleterious effect of SRZ on the LCF strength of coated MC-NG at 950°C.
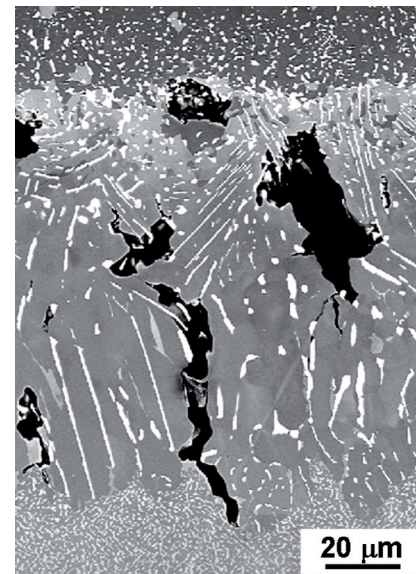

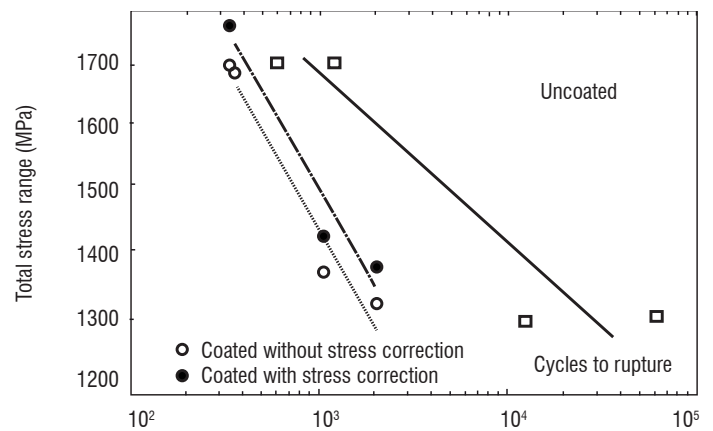Figure 15 - Secondary reaction zone in coated MC-NG after 199 hours of creep at 1050°C.

Figure 16 - LCF strength at 650°C of <001> SC specimens of the MC-NG alloy (R = -1; f = 0.33 Hz).
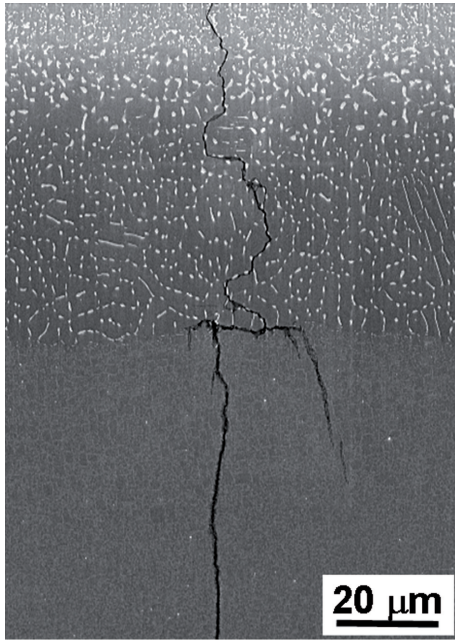
Figure 17 - Crack propagation through the SRZ and the γ-γ' structure of a NiAlPt-coated MC-NG LCF specimen having failed at 650°C (1070 cycles) (longitudinal section; SEM in backscattered electron mode).
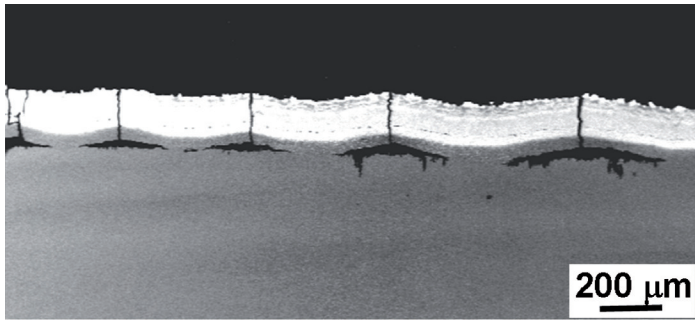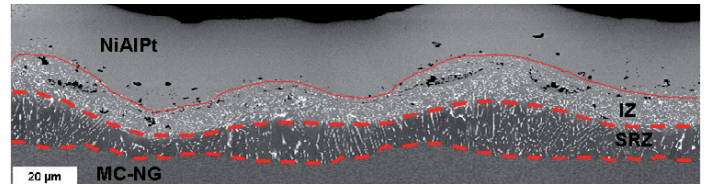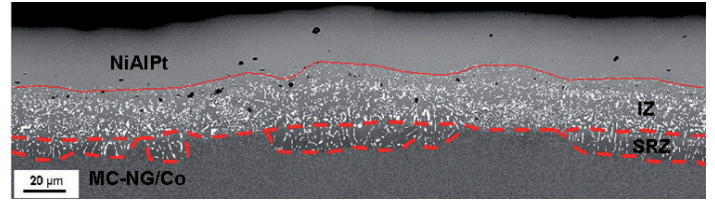

Figure 18 - Secondary cracks within the coating layer of a MC-NG LCF specimen having failed at 950°C (7010 cycles) (longitudinal section; SEM in backscattered electron mode).

Figure 19 - Interaction zones between: (a) the reference MC-NG superalloy or (b) the Co-modified one and a NiAlPt coating (IZ: primary interdiffusion zone; SRZ: secondary reaction zone).
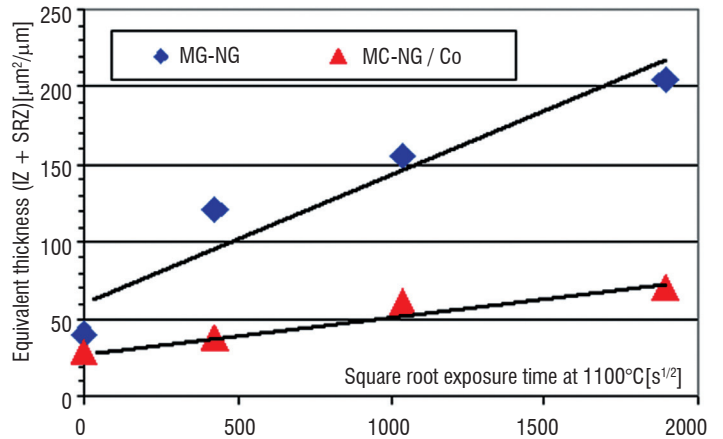

Figure 20 - Changes in the interdiffusion zone thickness over time, at 1100°C, in reference and Co-modified MC-NG alloys.

One solution generally considered for reducing SRZ proneness is to adapt the alloy substrate chemistry to the bond coat. Analysis of the results obtained for various superalloys (AM1, MC-NG, CMSX-4, CMSX-10M, Alloy 5A, René N6 and Alloy 11) coated with a platinum modified aluminide, puts forward hypotheses about the role of some elements in the SRZ occurrence frequency [33]. Thus, the presence of rhenium seems to be necessary, but not sufficient, for SRZ development. On the contrary, cobalt is inferred to play an inhibitive role. In addition, this element is known to improve the microstructural stability of rhenium-bearing superalloys, by reducing their sensitivity to precipitation of brittle intermetallic phases [32]. In order to validate this alleged effect of cobalt on SRZ mitigation and to analyze the corresponding mechanisms, a modified version of the MC-NG alloy was prepared by replacing 10 wt. % of nickel by the same amount of cobalt, an element that was originally absent from the alloy (table 1) [33, 35, 36]. SC samples were fully solution heat-treated prior to coating. Comparison between the base alloy and the modified one, both having been coated with a γ-NiAl(Pt) single phase coating, indeed shows a very significant decrease of the SRZ amount when cobalt is present in he substrate (figure 19).

Moreover, microstructural assessments of the interdiffusion zones after aging treatments, at temperatures within the 950-1100°C range, in an argon atmosphere, show that the SRZ growth rate as a function of temperature or of time is slower in the cobalt-bearing alloy (figure 21). This growth rate is controlled by diffusion as shown by the linear dependence of the SRZ thickness on the square root of time. The estimated diffusion coefficient is about 6.10^{-15} [m^2.s^{-1}] for the MC-NG alloy, which is very close to the value obtained for Alloy 5A [28]. This is about one order of magnitude lower for the Co-modified MC-NG alloy.

Conclusions

Various studies on nickel-based superalloys for SC turbine blade applications have shown the complex relationships between the chemistry, the physical characteristics, the microstructure and the mechanical behavior of such materials in a wide temperature range. In particular, the creep behavior is highly dependent on the size and morphology of the strengthening γ' precipitates, which in turn depend on the chemistry and change with time and temperature. Accurate

analyses of deformation mechanisms and microstructural changes through the use of both SEM and TEM techniques make it possible to propose hypotheses to explain the observed effects. Since these single crystal turbine blades need to be protected against environmental and thermal attacks by using adequate coatings, attention was also paid to the interactions between the substrate and a diffusion protective coating. The microstructure modifications due to the inter-diffusion processes were shown to be significant in the highly-alloyed single crystal superalloys recently developed for high temperature applications. This has a deleterious impact on creep strength, but the phenomenon can be reduced by modifying the alloy chemistry. All these studies therefore provide precious information useful for designing new superalloy compositions suited for specific applications in aircraft or land-based gas turbine engines ■

References

[1] P. CARON, T. KHAN - *Third Generation Superalloys for Single Crystal Turbine Blades*. Materials for Advanced Power Engineering 1998 - Part II, Forschungzentrum Jülich Gmbh, Jülich, Germany (J. Lecomte-Beckers, F. Schubert and P.J. Ennis, eds), pp. 897-912, 1998.

[2] P. CARON - *High γ' solvus New Generation Nickel-Based Superalloys for Single Crystal Turbine Blade Applications*. Superalloys 2000, TMS, Warrendale, PA, USA (T.M. Pollock et al., eds), pp. 737-746, 2000.

[3] P. CARON, J.-L. RAFFESTIN, S. NAVEOS - *Superalliage monocristallin à base de nickel à haut solvus γ'*. French patent, N°98 08 693, 7 July 1998.

[4] M. MORINAGA, N. YUKAWA, H. ADACHI and H. EZAKI - *New PHACOMP and its Application to Alloy Design*. Superalloys 1984, TMS-AIME, Warrendale, PA, USA (M. Gell et al., eds), pp. 523-532, 1984.

[5] P. CARON, S. NAVEOS and T. KHAN - *Improvement of the Cyclic Oxidation Behaviour of Uncoated Nickel Based Single Crystal Superalloys*. Materials for Advanced Power Engineering 1994 - Part I, Kluwer Academic Publisher, Dordrecht, Holland (D. Coutsouradis et al., eds), pp. 1185-1194, 1994.

[6] D. ARGENCE, C. VERNAULT, Y. DESVALLEES and D. FOURNIER - *MC-NG: A 4th Generation Single-Crystal Superalloy for Future Aeronautical Turbine Blades and Vanes*. Superalloys 2000, TMS, Warrendale, PA, USA (T.M. Pollock et al., eds), pp. 829-837, 2000.

[7] R.F. SINGER - *New Materials for Industrial Gas Turbines*. Mat. Sci. Techn., Vol. 3, pp. 726-732, 1987.

[8] T. KHAN and P. CARON - *Development of a New Single Crystal Superalloy for Industrial Gas Turbine Blades*. High Temperature Materials for Power Engineering 1990, Kluwer Academic Publishers, Dordrecht, Holland (E. Bachelet et al., eds), pp. 1261-1270, 1990.

[9] P. CARON, A. ESCALE, G. McCOLVIN, M. BLACKER, R. WAHI and L. LELAIT - *Development of New High Strength Corrosion Resistant Single Crystal Superalloys for Industrial Gas Turbine Applications*. PARSONS 2000 - Advanced Materials for 21st Century Turbines and Power Plant, IOM Communications Ltd, London, UK (A. Strang et al., eds), pp. 847-864, 2000.

[10] P. CARON, M. BLACKLER, A. ESCALE, G. McCOLVIN, P. WAHI and L. LELAIT - *Nickel-Based Superalloy Having a Very High Resistance to Hot-Corrosion for Monocrystalline Blades of Industrial Turbines.* European Patent Application EP 1 211 335 A1, 30 November 2000.

[11] P. CARON, M. BLACKLER, A. ESCALE, G. McCOLVIN, P. WAHI, L. LELAIT - *Nickel-Based Superalloy Having a High Resistance to Hot-Corrosion for Mono-Crystalline Blades of Industrial Turbines.* European Patent Application EP 1 211 336 A1, 30 November 2000.

[12] A. SATO, Y.-L. CHIU and R.C. REED - *Oxidation of Nickel-based Single-crystal Superalloys for Industrial Gas Turbine Applications*. Acta mater., Vol. 59, pp. 225-240, 2011.

[13] F. DIOLOGENT and P. CARON - *On the Creep Behavior at 1033 K of New Generation Single-Crystal Superalloys*. Mat. Sc. Eng. A, Vol. 385, N°1-2, pp. 245-257, 2004.

[14] P. CARON and T. KHAN - *Improvement of Creep Strength in a Nickel-Base Single-Crystal Superalloy by Heat-Treatment*. Mat. Sc. Eng., Vol. 61, pp. 173-194, 1983.

[15] U. GLATZEL and M. FELLER-KNIEPMEIER – *Calculations of Internal Stresses in the γ/γ' Microstructure of a Nickel-Base Superalloys with High Volume Fraction of γ' Phase*. Scripta Met., Vol. 23, pp. 1839-1844, 1989.

[16] P. CARON and F. DIOLOGENT - *Effect of the γ/γ' Lattice Mismatch on the Creep Behaviour at 760°C of New Generation Single Crystal Superalloys*. TMS 2008 Annual Meeting Supplemental Proceedings, Volume 3: General Paper Selections, TMS, Warrendale, USA, pp. 171-176, 2008.

[17] S. MA, L. CARROLL, T.M. POLLOCK - *Development of γ phase stacking faults during high temperature creep of Ru-containing single crystal superalloys*. Acta Mater., Vol. 55, pp. 5802-5812, 2007.

[18] R.A. HOBBS, L. ZHANG and C.M.F. RAE - *The effect of ruthenium on the intermediate to high temperature creep response of high refractory content single crystal nickel-base superalloy*. Mat. Sc. Eng. A, Vol. 489, pp. 65-76, 2008.

[19] N. TSUNO, K. KAKEHI and CMF RAE - *Effect of Ruthenium on Creep Strength of Ni-Base Single-Crystal Superalloys at 750°C and 750 MPa*. Met. Mater. Trans. A, Vol. 40A, pp. 269-272, 2009.

[20] P. CARON, M. BENYOUCEF, A. COUJOU, J. CRESTOU and N. CLEMENT - *Creep Behaviour at 1050°C of a Re-Containing Single Crystal Superalloy*. Proceedings of International Symposium on Materials Ageing and Life management (ISOMALM 2000), Allied Publishers Ltd., Chennai, India, (B. Raj, K.Bhanu, S. Rao, T.Jayakumar, R.K.Dayal, eds) pp. 148-156, 2000.

[21] H. HARADA, T. YAMAGATA, T. YOKOKAWA and M. YAMAZAKI - *Computer Analysis on Microstructure and Property of Nickel-Base Single Crystal Superalloys*. Proc. 5Th Int. Conf. on Creep and Fracture of Engineering Materials and Structures, IOM, London, UK (B. Wilshire, R.W. Evans, eds), pp. 255-264, 1993.

[22] J.K. ZHANG, T. MURAKAMO, Y. KOIZUMI, T. KOBAYASHI, H. HARADA and S. MAZAKI - *Interfacial Dislocation Networks Strengthening a Fourth-Generation Single-Crystal TMS-138 Superalloy*, Met. Mater. Trans. A, Vol. 33, pp. 3741-3746, 2002.

[23] P. CARON, C. RAMUSAT and F. DIOLOGENT - *Influence of the γ' Fraction on the γ/γ' Topological Inversion during High Temperature Creep of Single Crystal Superalloys*. Superalloys 2008, TMS, Warrendale, PA, USA (R.C. Reed, K.A. Green, P. Caron, T.P. Gabb, M.G. Fahrmann, E.S. Huron,S.A. Woodard, eds), pp. 159-167, 2008.

[24] P. CARON, F. DIOLOGENT and S. DRAWIN - *Influence of Chemistry on the Tensile Yield Strength of Nickel-Based Single Crystal Superalloys*. Advanced Materials Research, Vol. 278, pp. 345-350, 2011.

[25] F. DIOLOGENT - *Comportement en fluage et en traction de superalliages monocristallins à base de nickel*. Doctorate thesis, Université Paris XI, France, 2002.

[26] P. VEYSSIERE and G. SAADA - *Dislocations in Solids*. Vol. 10, Elsevier Sciences (F. Nabarro and M. Duesbery, eds), 1996.

[27] M. KARUNARATNE, P. CARTER and R.C. REED - *Interdiffusion in the Face-Centred Cubic Phase of the Ni-Re, Ni-Ta and Ni-W Systems between 900 and 1300°C*. Mater. Sci. Eng., A281, pp. 229-233, 2000.

[28] M. PESSAH, P. CARON and T. KHAN - *Effect of μ Phase on the Mechanical Properties of a Nickel-Base Single Crystal Superalloy.* Superalloys 1992, TMS, Warrendale, PA, U.S.A. (S.D. Antolovich et al., eds), pp. 567-576, 1992.

[29] M. PESSAH-SIMONETTI, P. CARON and T. KHAN - *Effect of a Long-Term Prior Aging on the Tensile Behaviour of a High-Performance Single Crystal Superalloy*. Journal de physique IV, Colloque C7, supplement of the Journal de Physique III, Vol. 3, pp. 347-350, 1993.

[30] M. SIMONETTI and P. CARON - *Role and Behaviour of μ Phase During Deformation of a Nickel-Based Single Crystal Superalloy*. Mat. Sc. and Engin., A254, pp. 1-12, 1998.

[31] W.S. WALSTON, J.C. SCHAEFFER and W.H. MURPHY - *A New Type of Microstructural Instability in Superalloys – SRZ*. Superalloys 1996, TMS, Warrendale, PA, USA (R.D. Kissinger et al., eds), pp. 9-18, 1996.

[32] O. LAVIGNE, C. RAMUSAT, S. DRAWIN, P. CARON, D. BOIVIN and J.-L. POUCHOU - *Relationships between microstructural instabilities and mechanical behaviour in new generation nickel-based single crystal superalloys*. Superalloys 2004, TMS, Warrendale, PA, USA (K. A. Green et al., eds), pp. 667-675, 2004.

[33] P. CARON, O. LAVIGNE, C. RAMUSAT, J. BENOIST and C. RIO - *Secondary reaction zones in coated single crystal superalloy*. Superalloys and Coatings for High Temperature Applications, TMS Annual Meeting 2005, San Francisco, CA, USA, 13-17 February 2005.

[34] S. WALSTON, A. CETEL, R. MACKAY, K. O'HARA, D. DUHL and R. DRESHFIELD - *Joint development of a fourth generation single crystal superalloy*, Superalloys 2004, TMS, Warrendale, PA, USA (K.A. Green et al., eds), pp. 15-24, 2004.

[35] O. LAVIGNE, J. BENOIST, P. CARON and C. RAMUSAT - *Interactions between 4th Generation Single Crystal Superalloys and an Aluminide Bond Coat*, Turbine Forum 2006: Advanced Coatings for High Temperature, Forum of Technology, Dorsten, Germany, 2006.

[36] O. LAVIGNE, P. CARON, C. RAMUSAT and D. BOIVIN - *Influence of Cobalt on the Interaction between a Fourth Generation Single Crystal Superalloy and Its Protective Coating*. TMS Annual Meeting 2007, Orlando, FL, USA, 25 February-1 March 2007.

Acronyms

SC (Single Crystal)
TCP (Topologically Close-Packed)
IGT (Industrial Gas Turbine)
APB (Antiphase Boundary)
ESRF (European Synchrotron Research Facility)
TEM (Transmission Electron Microscopy)
SEM (Scanning Electron Microscopy)
LCF (Low Cycle Fatigue)
YS (Yield Strength)
TBC (Thermal Barrier Coating)
EB-PVD (Electron Beam-Physical Vapor Deposition)
SRZ (Secondary Reaction Zone)
EBSD (Electron Backscattered Diffraction)
IZ (Interdiffusion Zone)
EDS (Energy Dispersive Spectroscopy)

AUTHORS

Pierre Caron obtained his doctoral degree in Metallurgy from the University of Paris XI - Orsay in 1979 and his Habilitation Degree in 2000 from the same University. Since 1980, he is involved in various studies on superalloys and high-temperature materials, including alloy design and studies of the relationships between chemistry, microstructure and mechanical behaviour. He is currently a senior scientist and special advisor in the field of superalloys in the Department of Metallic Materials and Structures.

Odile Lavigne graduated as a physicist engineer from the Ecole Supérieure de Physique et Chimie Industrielles in Paris and obtained a PhD degree in Material Science from the University of Paris VI. She joined Onera in 1986, where she was successively involved in developing stealth systems and high temperature composite materials for space applications. For the past fifteen years, she has been working as a senior scientist on thermal barrier systems for gas turbine engines.